PERGAMON

International Journal of Multiphase Flow 26 (2000) 977–998

International Journal of Multiphase Flow

www.elsevier.com/locate/ijmulflow

Mechanism of slug formation in downwardly inclined pipes

Bennett D. Woods, Evan T. Hurlburt, Thomas J. Hanratty*

Department of Chemical Engineering, University of Illinois, Urbana, IL 61801, USA

Received 21 January 1999; received in revised form 11 June 1999

Abstract

This paper examines the effect of small downward inclinations on the formation of slugs. Experiments were conducted with air and water at atmospheric pressure, in a pipe with a diameter of 0.0763 m, a length of 23 m and inclinations of −0.2, −0.5 and −0.8°. Measurements of the variation of the interfacial displacement were made simultaneously at a number of locations. For low gas velocities in a horizontal configuration waves with lengths of 16–20 cm, grow until they reach of the top of the pipe. These waves evolve from smaller wavelength waves (8–10 cm) through a non-linear growth mechanism. At high gas velocities, the liquid height is not large enough for this mechanism to be operable. In these cases slugs evolve from the coalescence of roll waves. Surprisingly, the large amplitude small wavelength waves observed in horizontal flows, at the transition to slug flow, are damped in pipelines that are inclined slightly downward. The transition is associated with the initiation of long wavelength, small amplitude waves, whose appearance is predicted by a viscous long wavelength linear stability analysis. A local Kelvin–Helmholtz instability at the crest of a growing long wavelength wave is observed when a slug forms. The frequency of slugging is equal to frequency of these long wavelength waves.

Keywords: Gas–liquid pipe flow; Slug flow; Stratified-slug flow transition; Pipe inclination; Slug frequency

1. Introduction

Slugging is a commonly observed pattern in horizontal and near horizontal concurrent gas–liquid flows. It is characterized by the intermittent appearance of highly aerated masses of

* Corresponding author. Tel.: +1-217-333-1318; fax: +1-217-333-5052.
E-mail address: hanratty@scs.uiuc.edu (T.J. Hanratty).

0301-9322/00/$ - see front matter
PII: S0301-9322(99)00075-0

liquid that fill the whole cross section of a pipe and travel approximately at the gas velocity. They are separated from one another by a stratified configuration. This paper examines the effect of small downward inclinations on the mechanism of slug formation. The motivation is to provide a better understanding of the influence of inclination on the transition from a stratified to a slug flow and on the frequency of slugging.

Considerable progress has been made in describing how an instability of a stratified flow can lead to the formation of slugs at a low gas velocity. Wallis and Dobbins (1973) explored the use of an inviscid linear stability analysis to predict the initiation of long wavelength waves. They found that the predicted critical gas velocity is approximately twice what is observed. Lin and Hanratty (1986a) and Wu et al. (1987) included viscous effects and found close agreement between the predicted critical gas velocity for the initiation of waves and the initiation of slugs at low gas velocities in an air–water system at atmospheric pressure. The analysis shows that the transition is best described by a plot of the influence of the superficial gas velocity, U_{SG}, on the critical height of the liquid layer, h, normalized by the pipe diameter, D. Larger U_{SG} are required to initiate an instability at smaller h/D. For very small h/D the transition to slug flow is not caused by the instability of a stratified flow; it is associated with the stability of a slug (Woods and Hanratty, 1996).

The picture that is evoked by the stability analyses is that very long wavelength waves grow until they reach the top of the pipe. Detailed observations of the interfacial behavior at the transition to slug flow were made by Fan et al. (1993a, 1993b). These revealed an appearance of small amplitude long wavelength waves. However, the slugs were observed to evolve from waves with lengths of 8–10 cm. These bifurcate through a resonance mechanism. The resulting 16–20 cm waves can grow and tumble or, if h/D is large enough, can grow to form a slug before they become saturated. These observations present a paradox in that the formation of slugs appears to occur by a different mechanism from what is suggested by the successful linear stability analysis.

The striking influence of small pipe inclinations on the transition to slug flow is documented in a number of studies. Barnea et al. (1980) examined air–water flows with upward inclinations of 0.25, 0.5, 1, 2, 5 and 10° and with downward inclinations of 1, 2, 5 and 10°. Andreussi and Persen (1987) carried out studies with air and water flowing in a 5 cm pipe which was inclined downward at 0.65° and 2.1° and Stanislav et al. (1986), with air and water flowing in a pipe with upward inclinations of 0–9°. Grolman et al. (1996) developed flow regime maps for upflows at angles between 0.1 and 6° in pipes with diameters of 0.026 and 0.051 m for air/water and air/tetradecane systems at atmospheric conditions. These studies show that higher liquid flow rates are required to produce slugs in downflows. For upflows, the opposite is the case; for an inclination of only $+1°$, the stratified region in a flow regime map shrinks to a very small bell-shaped area (Grolman et al., 1996).

These results have been interpreted with stability analyses for horizontal stratified flow by arguing that the critical h/D for a given U_{SG} would be the same in horizontal and inclined flows. For downflows this would require a larger liquid flow; for upflows, a smaller liquid flow. This approach has been used successfully by Barnea et al. (1980), Stanislav et al. (1986) and Kokal and Stanislav (1989). The results presented in this paper were obtained for smaller downward inclinations, 0.2, 0.5 and 0.8°, than had been studied previously. The experiments were performed in a pipeline with a diameter of 0.0763 m and a length of 23 m. Air/water

flows at atmospheric pressure were used. Liquid holdup measurements were made simultaneously at multiple locations along the pipe. A number of surprising results were obtained.

2. Theory

The classical inviscid Kelvin–Helmholtz analysis of a stratified flow considers an infinitesimal wave at the interface of two inviscid fluids which, for the case considered here, have a gas with velocity $\bar{U}$ and a liquid with velocity $\bar{u}$ (Milne-Thomson, 1968). If viscous effects are neglected, the following equation relates the wave velocity, C, to the wavenumber, $k = 2\pi/\lambda$, for flow between two parallel plates:

$$k\rho_L(\bar{u} - C)^2 \coth k\bar{h}_L + k\rho_G(\bar{U} - C)^2 \coth k\bar{h}_G = g\cos\theta(\rho_L - \rho_G) + \sigma k^2 \tag{1}$$

Here, $\bar{h}_G$ is the height of the gas layer, $\bar{h}_L$,the height of the liquid layer, ρ_G, the gas density, ρ_L, the liquid density, g, the acceleration of gravity, θ, the inclination angle, and σ, the surface tension. Instability occurs when the destabilizing effects of liquid inertia and gas phase pressure variations 180° out of phase with the wave height are larger than the stabilizing effects of gravity and surface tension. The wave velocity in Eq. (1) is complex,

$$C = C_R + iC_i \tag{2}$$

Waves will grow or decay depending on the sign of C_i. The condition $C_i = 0$ defines neutral stability, where Eq. (1) gives

$$(\bar{U} - \bar{u})^2 = \frac{\bar{h}_G}{\rho_G}\left[g\cos\theta(\rho_L - \rho_G) + k^2\sigma\right]\left[\frac{\tanh(k\bar{h}_G)}{k\bar{h}_G} + \frac{\rho_G}{\rho_L}\frac{\tanh(k\bar{h}_L)}{k\bar{h}_G}\right] \tag{3}$$

The real part of the wave velocity is

$$C_R = \frac{\bar{U}\rho_G\bar{h}_L + \bar{u}\rho_L\bar{h}_G}{\rho_L\bar{h}_G + \bar{h}_L\rho_G} \tag{4}$$

If one considers long wavelength waves, for which $k\bar{h}_L \ll 1$ and $k\bar{h}_G \ll 1$, and if ρ_G/ρ_L is considered to be small, Eqs. (3) and (4) simplify to the following relations for the initiation of an instability:

$$\rho_G(\bar{U} - \bar{u})^2 = \rho_L g\cos\theta\bar{h}_G \tag{5}$$

with

$$C_R \cong \bar{u} \tag{6}$$

Wallis and Dobbins (1973) found that Eq. (5) overpredicts the critical gas velocity, for the initiation of slugging, by a factor of about 2.

From Eqs. (1) and (6), it seen that the inviscid analysis predicts that liquid inertia is neither

stabilizing nor destabilizing. Lin and Hanratty (1986a, 1986b) and Wu et al. (1987) introduced the influence of a shear stress at the gas–liquid interface and a resisting stress at the wall. This produced values of C_R which are different from $\bar{u}$ and a destabilizing influence of liquid inertia.

Lin and Hanratty (1986a, 1986b) adapted this viscous analysis to the more complicated case of flow in a circular pipe. The simplified representation of the geometry presented by Govier and Aziz (1972) was used. The interface was assumed to be flat and to have a length of S_i. The lengths of the segments of the pipe circumference that are in contact with the gas and with the liquid are S_G and S_L. The areas covered by gas and liquid are A_G and A_L. The height at the center of the stratified liquid is h.

A plug flow is assumed. Because long wavelength waves are considered, a shallow water assumption is made, so that the pressure variation in the liquid at a given x-location is given by

$$p = P_i + \rho_L(h - y)g\cos\theta \tag{7}$$

where P_i is the gas phase pressure at the interface and p is the pressure in the liquid. The equations of conservation of mass and momentum are given as

$$\frac{\partial A_L}{\partial t} + \frac{\partial(uA_L)}{\partial x} = 0 \tag{8}$$

$$\frac{\partial(uA_L)}{\partial t} + \frac{\partial\left(u^2A_L\right)}{\partial x} = -\frac{A_L}{\rho_L}\left(\frac{\partial P_i}{\partial x} + \rho_L g\cos\theta\frac{\partial h}{\partial x}\right) + \frac{1}{\rho_L}(\tau_i S_i - \tau_w S_L) + A_L g\sin\theta \tag{9}$$

Here, u is the liquid velocity, τ_i is the stress at the interface and τ_w is the stress at that portion of the wall that is in contact with the liquid. The quantities in this equation are assumed to be given by the sum of mean and fluctuating contributions. Thus,

$$A_L = \bar{A}_L + \hat{A}_L \exp ik(x - Ct) \tag{10}$$

where k is the wavenumber, C is the complex wave velocity and $\hat{A}_L$ is the amplitude of the disturbance. Eq. (8) gives a relation between the amplitude of the fluctuations in the liquid velocity, $\hat{u}_L$, and $\hat{A}_L$

$$\hat{u}_L = (C - \bar{u})\frac{\hat{A}_L}{\bar{A}_L} \tag{11}$$

The flow is assumed to be fully-developed so that the time mean momentum balance is

$$0 = -\frac{\bar{A}_L}{\rho_L}\frac{\partial\bar{P}_i}{\partial x} + \frac{1}{\rho_L}(\bar{\tau}_i S_i - \bar{\tau}_w S_L) + \bar{A}_L g\sin\theta \tag{12}$$

If the disturbances are assumed small the following equation is obtained from Eqs. (8), (9), (11) and (12):

$$-ik(C-\bar{u})^2 = -\bar{A}_L \frac{ik}{\rho_L}\frac{\hat{P}_i}{\hat{A}_L} - \bar{A}_L ik \frac{\hat{h}}{\bar{A}_L} g\cos\theta + \frac{\bar{\tau}_w \bar{S}_L}{\rho_L \bar{A}_L} - \frac{\bar{\tau}_i \bar{S}_i}{\rho_L \bar{A}_L} + \frac{\bar{S}_i}{\rho_L}\frac{\hat{\tau}_i}{\hat{A}_L} - \frac{\bar{S}_L}{\rho_L}\frac{\hat{\tau}_w}{\hat{A}_L} + \frac{\bar{\tau}_i}{\rho_L}\frac{\hat{S}_i}{\hat{A}_L} - \frac{\bar{\tau}_w}{\rho_L}\frac{\hat{S}_L}{\hat{A}_L} \tag{13}$$

Here, $(\hat{h}/\hat{A}_L) = \mathrm{d}h/\mathrm{d}A_L$, $(\hat{S}_i/\hat{A}_L) = \mathrm{d}S_i/\mathrm{d}A_L$, and $(\hat{S}_L/\hat{A}_L) = \mathrm{d}S_L/\mathrm{d}A_L$. At neutral stability $C = C_R$ is real. The real and imaginary parts of Eq. (13) give two equations:

$$-\left(\frac{C_R}{\bar{u}} - 1\right)^2 = -\frac{\bar{A}_L}{\rho_L \bar{u}^2}\frac{\hat{P}_{iR}}{\hat{A}_L} - \frac{g\bar{A}_L\cos\theta}{\bar{u}^2}\frac{\hat{h}}{\hat{A}_L} + \frac{\bar{S}_i}{k\rho_L\bar{u}^2}\frac{\hat{\tau}_{iI}}{\hat{A}_L} - \frac{\bar{S}_L}{k\rho_L\bar{u}^2}\frac{\hat{\tau}_{wI}}{\hat{A}_L} \tag{14}$$

$$0 = \bar{A}_L k\frac{\hat{P}_{iI}}{\hat{A}_L} + \frac{\bar{\tau}_w\bar{S}_L}{\bar{A}_L} - \frac{\bar{\tau}_i\bar{S}_i}{\bar{A}_L} + \bar{S}_i\frac{\hat{\tau}_{iR}}{\hat{A}_L} - \bar{S}_L\frac{\hat{\tau}_{wR}}{\hat{A}_L} + \bar{\tau}_i\frac{\hat{S}_i}{\hat{A}_L} - \bar{\tau}_w\frac{\hat{S}_L}{\hat{A}_L} \tag{15}$$

Equations similar to Eqs. (8) and (9) can be written for the gas phase if a long wavelength assumption is made:

$$\frac{\partial A_G}{\partial t} + \frac{\partial(UA_G)}{\partial x} = 0 \tag{16}$$

$$\frac{\partial(UA_G)}{\partial t} + \frac{\partial\left(U^2A_G\right)}{\partial x} = -\frac{A_G}{\rho_G}\left(\frac{\partial P_i}{\partial x}\right) + \frac{1}{\rho_G}(-\tau_i S_i - \tau_B S_G) \tag{17}$$

where U is the gas velocity, A_G, the cross-sectional area occupied by the gas, τ_i, the interfacial stress and τ_B, the resisting stress on the portion of the wall bathed by the gas. A disturbance of the form

$$A_G = \bar{A}_G + \hat{A}_G \exp ik(x - Ct) \tag{18}$$

with $\hat{A}_G = -\hat{A}_L$ is introduced. Eq. (16) gives a relation between the amplitude of the fluctuations in the gas velocity and $\hat{A}_G$.

$$\hat{U} = -(\bar{U} - C)\frac{\hat{A}_G}{\bar{A}_G} = (\bar{U} - C)\frac{\hat{A}_L}{\bar{A}_G} \tag{19}$$

The following equations for $\hat{P}_{iR}$ and $\hat{P}_{iI}$ are obtained from Eqs. (17) and (19):

$$\frac{\hat{P}_{iR}}{\hat{A}_L} = \frac{\rho_G}{\bar{A}_G}\left[-\left(C_R - \bar{U}\right)^2 - \frac{\bar{S}_i}{\rho_G k}\frac{\hat{\tau}_{iI}}{\hat{A}_L} - \frac{\bar{S}_G}{\rho_G k}\frac{\hat{\tau}_{BI}}{\hat{A}_L}\right] \tag{20}$$

$$\frac{\hat{P}_{iI}}{\hat{A}_L} = \frac{1}{k\bar{A}_G}\left[\frac{\hat{\tau}_{iR}}{\hat{A}_L}\bar{S}_i + \frac{\hat{\tau}_{BR}}{\hat{A}_L}\bar{S}_G + \frac{\bar{\tau}_i\hat{S}_i}{\hat{A}_L} + \frac{\bar{\tau}_B\hat{S}_G}{\hat{A}_L}\right] + \frac{1}{k\bar{A}_G}\left[\frac{\bar{\tau}_i\bar{S}_i}{\bar{A}_G} + \frac{\bar{\tau}_B\bar{S}_G}{\bar{A}_G}\right] \tag{21}$$

where the mean momentum balance

$$\bar{A}_G \frac{\partial \bar{P}_i}{\partial x} = -\bar{\tau}_i \bar{S}_i - \bar{\tau}_B \bar{S}_G \tag{22}$$

was used to eliminate the mean pressure gradient.

For the range of conditions considered in this paper Eqs. (14) and (20) give

$$0 = \rho_L (C_R - \bar{u})^2 + \frac{\bar{A}_L}{\bar{A}_G} \rho_G \left(\bar{U} - C_R\right)^2 - g \bar{A}_L \rho_L \cos\theta \frac{\hat{h}}{\hat{A}_L} \tag{23}$$

where $(\bar{U} - C_R) \cong \bar{U}$ and $(\hat{A}_L/\hat{h}) = \mathrm{d}A_L/\mathrm{d}h$. Eq. (23) defines a critical gas velocity, $\bar{U}$, for the initiation of a long wavelength disturbance. The first term represents the destabilizing effect of liquid inertia and the third, the stabilizing effect of gravity. For an inviscid flow, $C_R = \bar{u}$ and liquid inertia has no influence. However, for very long wavelength waves the stresses, τ_i, τ_w and τ_B need to be considered in order to obtain a wave velocity to substitute into Eq. (23).

Therefore, the wave velocity, C_R, in Eq. (23) is calculated from Eqs. (15) and (11). The terms $\hat{\tau}_{iR}$, $\hat{\tau}_{wR}$, and $\hat{\tau}_{BR}$ are obtained by making the pseudo-steady state assumption, that the same relation for τ_i and τ_B exists both for the disturbed and undisturbed flows:

$$\tau_w = \frac{1}{2} \rho_L f_L u^2 \qquad \tau_B = \frac{1}{2} \rho_G f_G U^2 \tag{24}$$

where f_L and f_G are given by the Blasius equation

$$f_L = 0.0791 Re_L^{-1/4} \qquad f_G = 0.0791 Re_G^{-1/4} \tag{25}$$

The Reynolds numbers are defined by

$$Re_L = \frac{D_L \bar{u}}{\nu_L} \qquad Re_G = \frac{D_G \bar{U}}{\nu_G} \tag{26}$$

where D_L and D_G are hydraulic diameters,

$$D_L = \frac{4A_L}{S_L} \qquad D_G = \frac{4A_G}{S_G + S_i} \tag{27}$$

The relation for τ_i is

$$\tau_i = \frac{1}{2} \rho_G f_i \left(\bar{U} - C_R\right)^2 \tag{28}$$

The interfacial friction factor, f_i, can be larger than the friction factor for a smooth surface, f_s , which is given by Eq. (25). Wave velocities obtained in this way are similar to what is found for the kinematic waves defined by Lighthill and Whitham (1955). Details of this analysis may be found in the paper by Lin and Hanratty (1986a).

3. Experiments

3.1. Flow facility

The pipeline used in this study was constructed from Plexiglas to allow visual observations. The pressure at the outlet was atmospheric. The air flow was forced through an orifice located 5 pipe diameters upstream of the entry section. The velocity of the air through this orifice approaches the local velocity of sound. Consequently, downstream variations in the gas phase pressure caused by the formation of slugs do not strongly affect the inlet air flow.

Measurements of the variation of the liquid holdup and wave properties were obtained with a liquid conductance technique. A probe, consisting of two chromel wires, traverses the diameter of the pipe vertically. When a signal is applied to one of the wires, the conductance between the two wires is dependent upon the volume fraction of liquid between the wires. Each conductance wire was calibrated individually to compensate for differences in probe construction. Conductance measurements were converted into an equivalent h/D, where h is the liquid height at the bottom of the pipe.

Pressure fluctuations associated with the passage of a slug were measured using a piezoresitive pressure transducer mounted flush with the wall. A characteristic pressure pulse reveals the passage of a slug, as described by Lin and Hanratty (1986b) and Fan et al. (1993a, 1993b). This method of identifying slugs is useful at large gas velocities where the liquid is highly aerated and measurements from conductance probes cannot distinguish large amplitude waves from slugs.

The conditions required to initiate slug flow were investigated for $1 < U_{SG} < 7$ m/s in a 0.0763 m diameter pipe for downwardly inclined flows. The mechanism designed by Williams (1990) could incline the pipeline between $+2$ and -2° from the horizontal with a high degree of accuracy. The pipeline was supported at a number of locations by pipe racks attached to a 90 ft. beam. The beam was supported by a series of lifting stations and a stationary pivot point at one end of the beam. Each lifting station consisted of a support bed, a pair of screw jacks, and a pair of rollers. The rollers support the beam and allow the point of contact between the roller and the beam to change once the beam is inclined. The five lifting stations were synchronized so that the beam remains straight as it is inclined. This is accomplished by a gear system, powered by a single 0.25 HP AC motor, that drives each lifting station at a rate necessary to keep the beam straight.

It is imperative that the pipe segments supported by pipe racks are the same distance from the beam. The racks were first adjusted to be at the same height. Then, the leveling is improved by introducing a wavy stratified flow into the pipeline and adjusting the heights of the pipe racks so that no hydraulic gradients exist. Of particular concern are gradients that may occur at the connection of two pipe segments, since large amplitude interfacial waves experience a noticeable change in wave velocity as the waves translate through a misaligned pipe section.

Williams (1990) used a simple pipe tee to contact the air and water at the beginning of the pipeline, where water was introduced in the run and air was introduced in the branch. When the pipeline was declined, this method of introducing the phases resulted in large flow disturbances inside the pipe tee at flow conditions necessary to produce slugging. The initiation

of slugs from disturbances originating inside the pipe tee was suppressed by elevating the entry section above the height of the rest of the pipe segments. Williams found this to be effective in eliminating disturbances for declinations up to 0.2°. For larger declinations, the liquid flow required to initiate slugging was too large for this procedure to dampen inlet disturbances. As a result, all the slugs at large declinations were found to be initiated very close to the entry.

These observations by Williams (1990) motivated the use of the mixing section shown in Fig. 1. An insert of height h_{insert} separates the two phases until the first pipe segment at $L/D = 0$ is reached. The insert is tapered at a small angle. Five entry sections were constructed, each with a different value of h_{insert}. When the pipeline is operated with a slug flow, an entry was chosen that introduced the liquid flow at the approximate height required to initiate slugging at the prevailing flow conditions. This prevents hydraulic gradients downstream of the entry; i.e., the height of liquid is approximately constant throughout the pipeline for flow conditions close to the transition to slug flow.

The conductance probes were located at $L/D = 4$, 60, 106, 140, 190, and 192. Measurements of wave velocities of small wavelength waves were determined from measurements with two probes that were 0.152 m apart at the end of the pipline, at $L/D = 190$ and 192. Wave velocities of long wavelength waves were determined by examining the cross correlation functions of wave height measurements from probes separated by a longer distance. The pressure fluctuations in the gas flow were measured with a pressure transducer at $L/D = 142$. The passage of a slug is associated with a large increase in the gas phase pressure.

4. Results

4.1. Effect of pipe declination on transition lines

Fig. 2 shows the effect of declination on the stratified-slug transition for downflows. The inlet pictured in Fig. 1 was used. The open circles denote the liquid flow required to initiate a

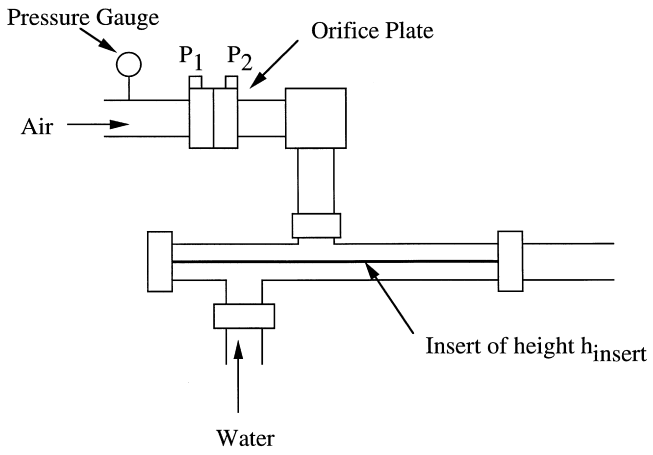

Fig. 1. Inlet design used in declination studies.

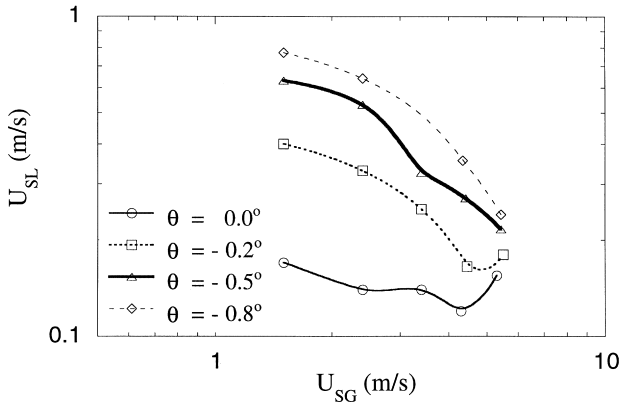

Fig. 2. Stratified-slug flow transition boundaries for horizontal flow and downflows.

slug at the end of the pipeline for horizontal flow. As the declination increases, the liquid flow required to initiate slugging increases. At low gas velocities, the critical liquid flow in a pipe with $\theta = -0.8^\circ$ is approximately four times the value for a horizontal pipeline. This shows that gravity plays a dominant role at low gas velocities. At $U_{SG} > 5$ m/s, the transition is weakly sensitive to declination, suggesting that the inertial effects of the gas flow overcome the stabilizing effects of gravity.

For all of the experiments in Fig. 2, the flow at the end of the pipe was well developed. Fig. 3 provides measurements of the mean h/D over the length of the pipeline at the onset to slug flow when $U_{SG} = 2.4$ m/s. The liquid was introduced at the inlet with $h/D = 0.60$. Each of the declined flows became well developed close to the entry, as indicated by the small changes in the liquid layer height after $L/D = 30$.

The increase in pipe declination is accompanied by an increase in the height of liquid required to initiate slugging, as indicated in Fig. 4. For constant U_{SG}, a large increase in the critical height, h_s, is observed when the pipe is declined from the horizontal to $\theta = -0.2^\circ$. The

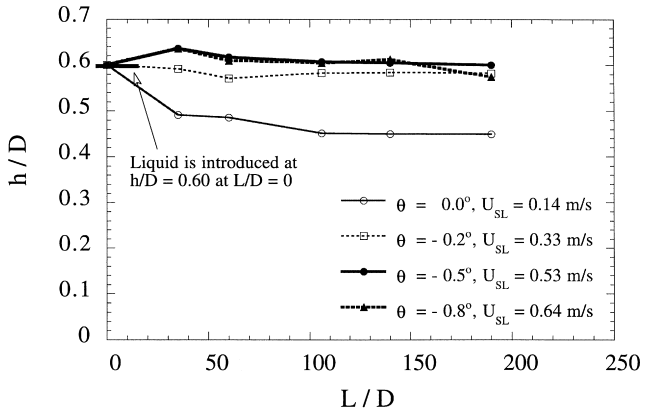

Fig. 3. Mean liquid height as a function of distance from the inlet and pipe inclination at the onset to slugging ($U_{SG} = 2.4$ m/s).

critical U_{SG} is not the same as for horizontal flows at the same h/D, as was presupposed by the authors. Declination is seen to stabilize the liquid layer. For $U_{SG} > 5$ m/s, h_s is insensitive to pipe inclinations between $\theta = 0.0^\circ$ and -0.8°.

4.2. Effect of pipe declination on wave properties at the transition to slug flow

4.2.1. Low gas velocities

For horizontal air–water flows, the interface at the onset to slug flow is characterized by large amplitude regular waves. The properties of these waves are documented by Fan et al. (1993a, 1993b). At low gas velocities, prior to the initiation of slugs, these regular waves have a frequency of 5 Hz, a wavelength of 15–20 cm and amplitudes of 1–2 cm. As the pipeline is declined, the gas–liquid interface is smoother at the transition to slug flow. Fig. 5 compares conductance measurements for a 10 s period at $L/D = 190$ for three different declinations, at the transition to slug flow for $U_{SG} = 1.6$ m/s. The measurements for a horizontal flow show the waves observed by Fan et al. The interface is much smoother for inclinations of -0.2 and -0.5°.

Fig. 6 presents wave spectra obtained at different distances from the inlet for a horizontal stratified flow at $U_{SG} = 1.6$ m/s and $U_{SL} = 0.17$ m/s. The power spectral density function $G_{xx}(f)$ is defined as

$$G_{xx}(f) = \frac{2}{T} E\left[|S_x(f)|^2\right] \tag{29}$$

where the quantity $S_x(f)$ is the finite Fourier transform

$$S_x(f) = \frac{1}{2\pi} \int_0^T h(t) \mathrm{e}^{-i2\pi ft}\, \mathrm{d}t \tag{30}$$

and T is the period of the wave height time series $h(t)$. The spectral functions in Fig. 6, and subsequent figures, are normalized with the mean square, ψ^2, of the time series. At $L/D = 60$,

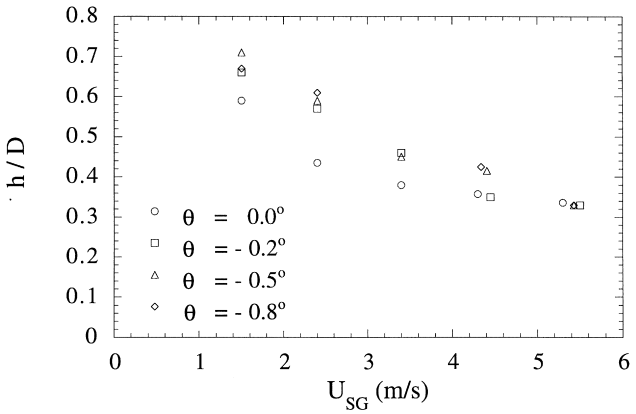

Fig. 4. Mean liquid height at the onset to slug flow as a function of U_{SG} and inclination.

most of the energy resides in waves with frequencies of 10–12 Hz. As these waves translate downstream, they resonate with waves with half their frequency. The outcome of this process is a wave with a frequency of 5–6 Hz at the end of pipe. This wave can become unstable and develop into a slug if the liquid layer is thick enough.

Fig. 7 presents wave spectra for stratified flows before the onset to slug flow when the pipe is declined. The gas velocity is the same as for the data, in Fig. 6, for $U_{SG} = 1.6$ m/s. The wave instability mechanism documented by Fan et al. is not observed, in that the wave energy is evenly distributed over a large range of frequencies, 0.1–7.0 Hz.

Fig. 8 shows conductance results for a slug flow for $\theta = -0.5^\circ$, $U_{SG} = 2.4$ m/s and $U_{SL} = 0.59$ m/s. The measurements are shown for a 50 s duration at $L/D = 35$, 60, 106, 190. For this flow condition, slugs are initiated periodically in the middle of the pipeline ($L/D \approx 106$–140). The measurements at $L/D = 190$ show that six slugs pass this station in 50 s; i.e., $f_s = 0.12$ s^{-1}. The y-axis for the measurements at $L/D = 35$ and 60 shows heights between $h/D = 0.5$ to 0.75. A low frequency, small amplitude wave is observed at $L/D = 60$. The vertical arrows indicate the crests of these waves. Six crests are observed in 50 s; the frequency of this long wavelength wave equals the frequency of slugging observed downstream. It should be noted that the liquid flow is supercritical, $Fr_L = 1.4$; the long wavelength waves are not propagating upstream as

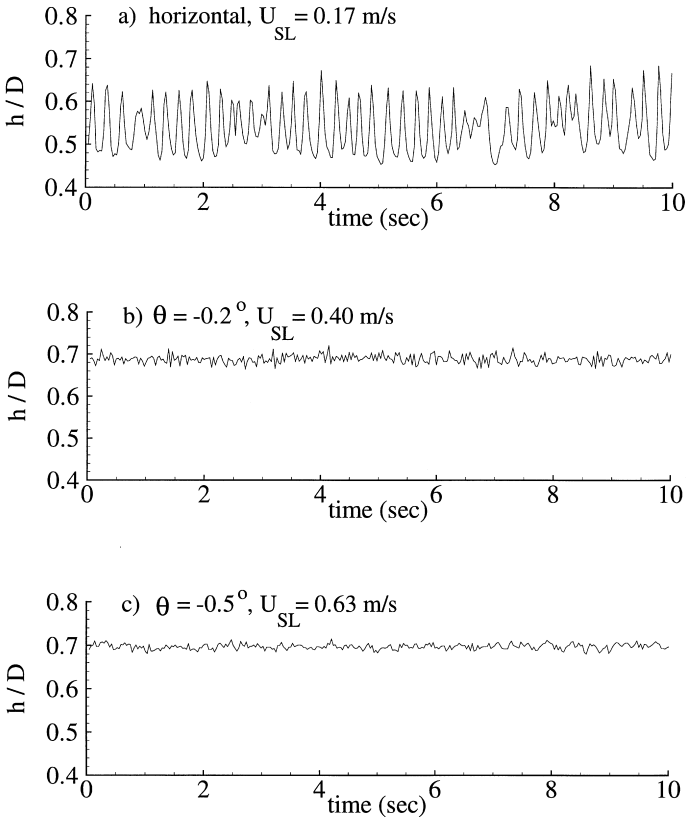

Fig. 5. Effect of inclination on the wave height measurements at $L/D = 190$ for $U_{SG} = 1.6$ m/s.

depression waves associated with slug formation, as observed in horizontal flows at low gas velocities; that is, $Fr_L < 1$ (Woods, 1998). The $f_s = 0.12$ s^{-1} wave in Fig. 8 is translating approximately at 1.5 m/s. The calculated correlation function between $L/D = 60$ and 106 is shown in Fig. 9. Since the two peaks in Fig. 9 are separated by 9 s, $\lambda \cong 12$ m.

The slugs shown in Fig. 8 originate from interfacial disturbances propagating periodically downstream. The long wavelength waves grow in amplitude until a local instability develops at a crest. An example of this behavior is given in Fig. 10, which shows eight images obtained from a video camera. Each of the images was obtained approximately 1/30th of a second after the prior image. These photographs cover a small length compared to the λ of 12 m. Consequently, the crest appears as a flat surface. The interface in Fig. 10(a) is smooth. A small wavelength instability, observed at the far right in the second frame, is seen to grow in amplitude in Fig. 10(c) and (d). This instability forms a slug in Fig. 10(f) and (h). Slugs are thus suggested to be the result of a local instability that develops at the crest of a long

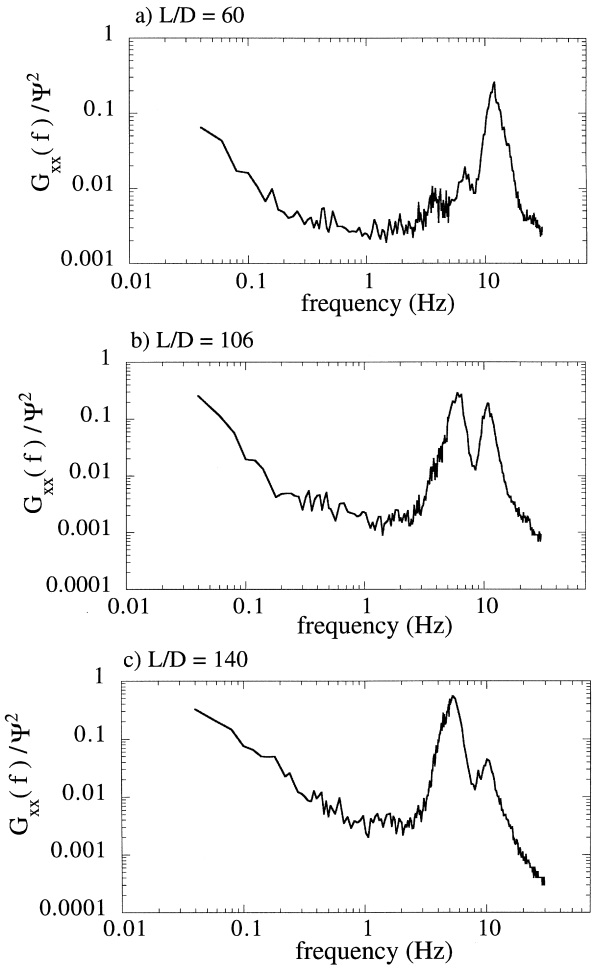

Fig. 6. Measurements of $G_{xx}(f)$ at $L/D = 60$, 106, and 140 for $U_{SG} = 1.6$ m/s, $U_{SL} = 0.17$ m/s, and $\theta = 0.0^\circ$.

wavelength wave. This mechanism was observed in channel flow experiments by Kordyban (1985) and by Kordyban and Ranov (1970), who photographed the initiation of slugs triggered by mechanically generated long wavelength waves.

4.2.2. High gas velocities

Fig. 11 presents measurements, for $U_{SG} = 4.4$ m/s and a liquid flow close to that needed for the onset of slugging, of the liquid holdup at $L/D = 190$ for four different declinations. Many large amplitude waves exist on the gas–liquid interface for the $\theta = 0.0^\circ$ and -0.2°. However, for $\theta = -0.5^\circ$ and -0.8° the interface is much smoother. For the horizontal flow, the 5 Hz small wavelength waves that are responsible for the formation of slugs at low gas velocities are observed to exist at the beginning of the pipeline. However, the liquid height at this U_{SG} ($h/D \approx 0.35$) is not large enough for these waves to grow into a slug. The wave crests tumble and form roll waves as they propagate downstream. A concentration of wave energy at 5–6 Hz

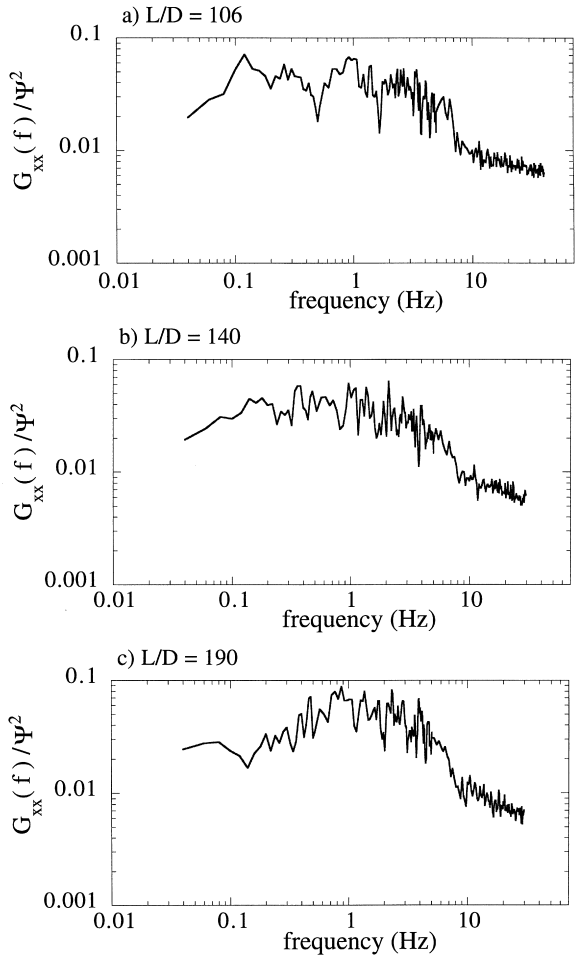

Fig. 7. Measurements of $G_{xx}(f)$ at $L/D = 106$, 140, and 190 for $U_{SG} = 1.6$ m/s, $U_{SL} = 0.63$ m/s, and $\theta = -0.5^\circ$.

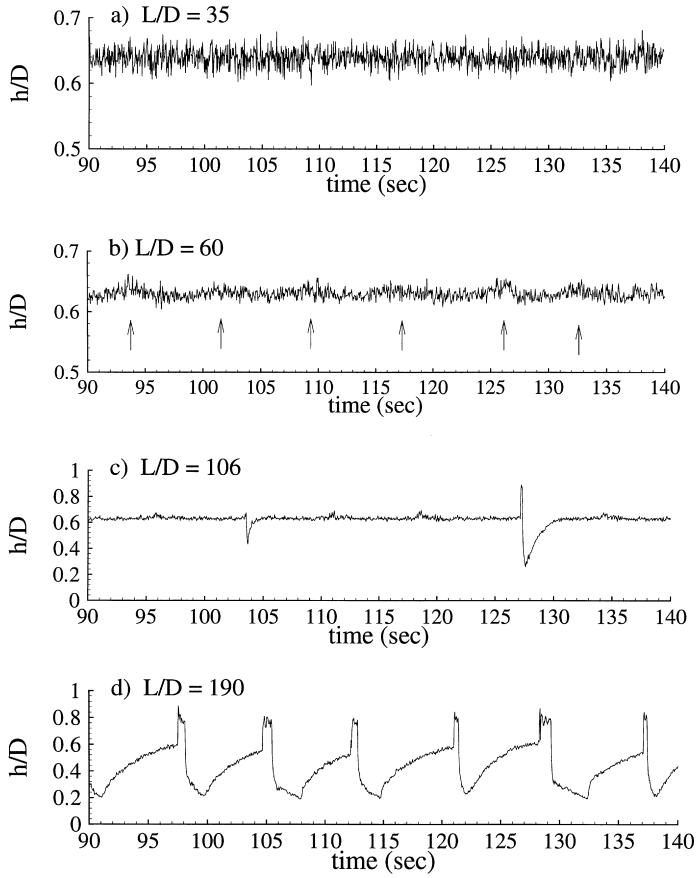

Fig. 8. Liquid holdup measurements at $U_{SG} = 2.4$ m/s and $U_{SL} = 0.59$ m/s for $\theta = -0.5^{\circ}$.

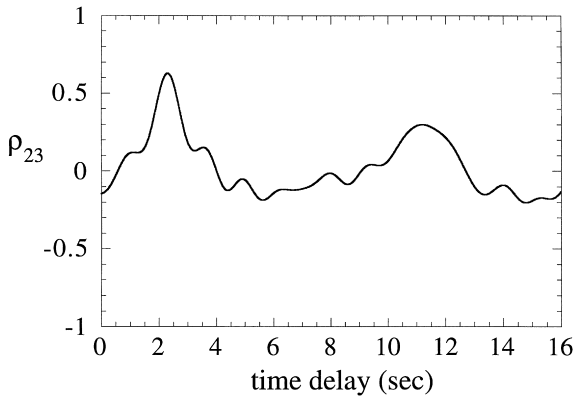

Fig. 9. Correlation function between liquid holdup profiles at $L/D = 60$ and 106 at $U_{SG} = 2.4$ m/s and $U_{SL} = 0.59$ m/s for $\theta = -0.5^{\circ}$.

is not observed in spectra at $L/D = 106$ and 140. The initiation of slugging in a horizontal pipe under these conditions is associated with the coalescence of roll waves (Fan et al., 1993a, 1993b; Woods and Hanratty, 1996). The interface for $\theta = -0.5^\circ$ and -0.8° is smooth.

As the gas velocity is increased, the effect of declination upon the wave structure becomes less. This is illustrated in Fig. 12 for $U_{SG} = 5.5$ m/s at a liquid velocity near the onset of slug flow. Roll waves are observed for horizontal flow and for all inclinations.

5. Discussion

It is surprising that the large amplitude, small wavelength waves observed at the onset to slug flow in a horizontal pipe are not observed at the onset of slug flow for $\theta < -0.2^\circ$. At this time, the reason for this behavior is not understood. However, an explanation needs to take

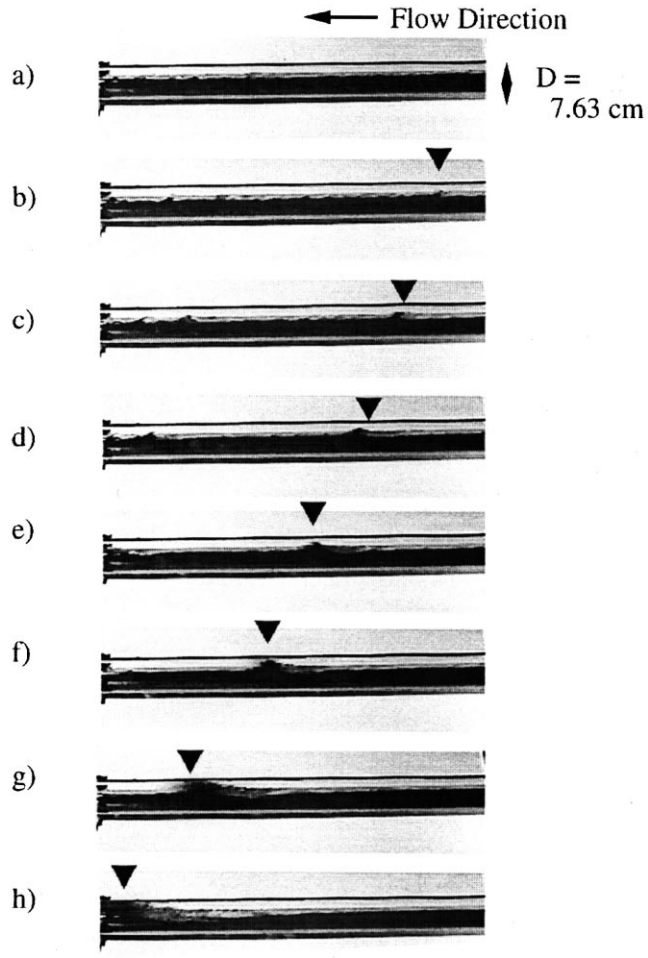

Fig. 10. Initiation of a slug at $U_{SG} = 2.4$ m/s, $U_{SL} = 0.59$ m/s for $\theta = -0.5^\circ$.

into consideration that flows in inclined pipes, at a fixed U_{SG} and h/D, differ from flows in horizontal pipes in that the liquid velocity is larger. This will be associated with a larger wave velocity and a larger wall resistance.

The results show that both long wavelength and small wavelength waves play roles in the initiation of slugs in downflows. Visual observations and experimental data suggest that the slugs evolve from small wavelength waves that suddenly form at the crests of slowly growing long wavelength waves. The small wavelength waves (≈ 2 cm) are affected by both gravity and surface tension. Consequently, the stability of these waves should be given by a classical Kelvin–Helmholtz analysis. The curves in Fig. 13 were calculated by solving the inviscid neutral stability relations, (3) and (4), along with the equations describing the equilibrium condition for a stratified flow. The neutral stability curves in Fig. 13(a) show a critical U_{SG} at which a wavelength of approximately 1–3 cm becomes unstable. This critical wavelength is relatively insensitive to h/D; it corresponds to a critical current velocity ($\bar{U} - \bar{u}$), of approximately 6.9 m/s, that is insensitive to the height of the liquid (Fig. 13(b)). The video images in Fig. 10 show a small amplitude wave, whose wavelength is approximately 2 cm,

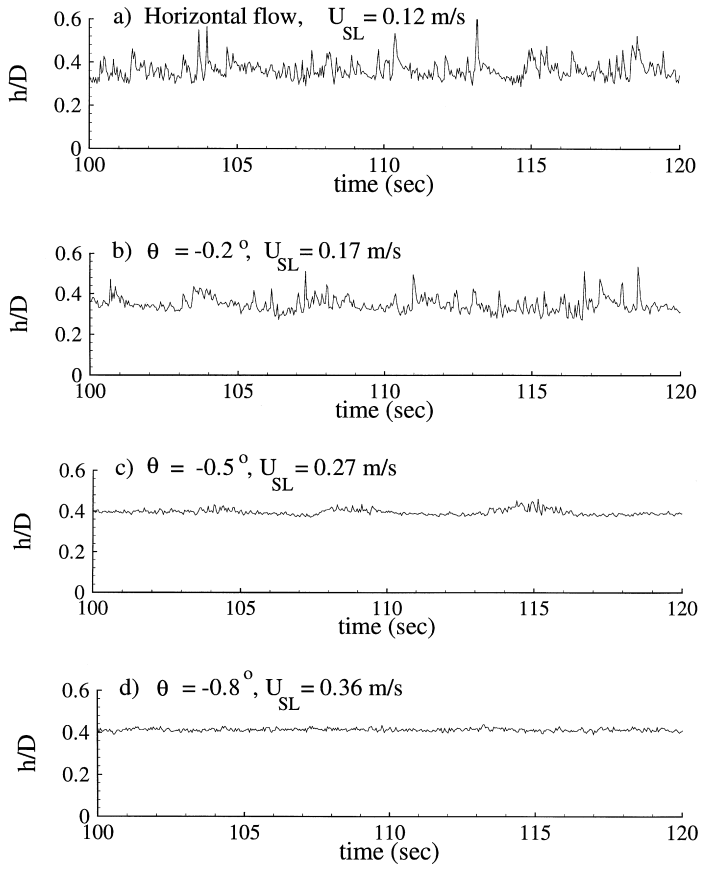

Fig. 11. Effect of pipe inclination upon the liquid holdup measurements at $L/D = 190$ at the onset to slug flow for $U_{SG} = 4.4$ m/s.

becoming unstable. The dimensionless height at the crest of the long wavelength, shown in Fig. 8, is $h/D = 0.64$. For this height, $\bar{U}$ and $\bar{u}$ are 7.5 and 0.87 m/s. The value of $\bar{U} - \bar{u}$ at the crest of the long wavelength waves roughly corresponds to the critical current velocity needed to produce a classical KH instability.

Fig. 14(a) compares theoretical values of h/D at neutral stability with experimental data for $\theta = -0.5^\circ$. The thick dashed curve is the prediction for a classical KH instability. A wavelength of 1.5 cm is used in this calculation since this is the most unstable wave (Fig. 13). The prediction of Taitel and Dukler (1976) is given by the dotted curve. Results from the long wavelength viscous analysis of Lin and Hanratty (1986a, 1986b) in Section 2, are given by the solid line. The ratio f_i/f_s in the viscous analysis is taken to be unity. For small gas velocities, a lower h/D is required to produce unstable long wavelength viscous waves than is required for small wavelength inviscid KH waves. Long wavelength waves are observed for stratified flow prior to the appearance of slugs, as indicated by the results in the previous section.

Even though slug formation occurs through a local inviscid KH instability, this theory does not accurately predict transition boundaries; the predicted value of U_{SL} at the transition to

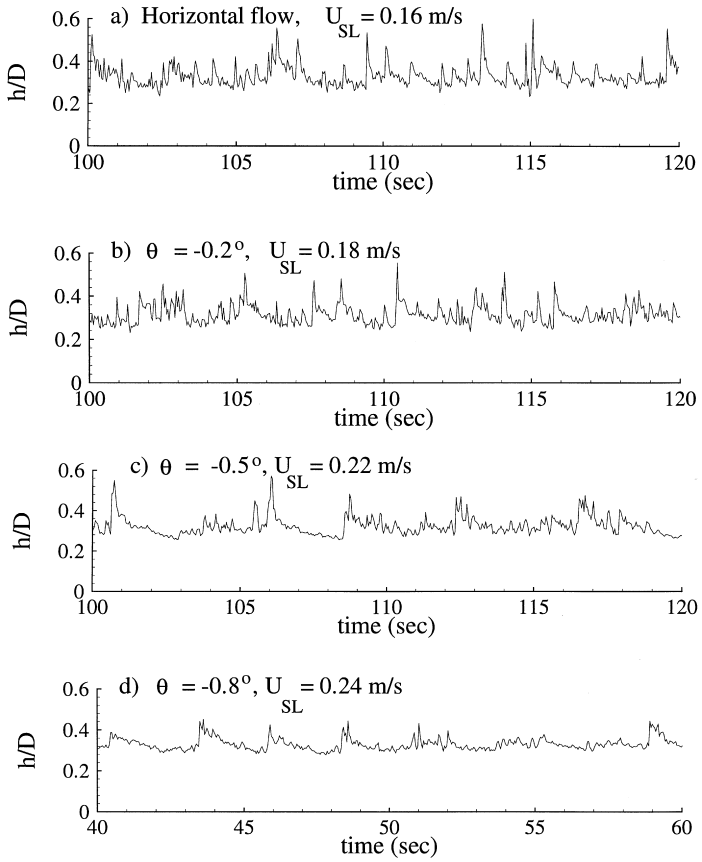

Fig. 12. Effect of inclination upon the liquid holdup measurements at $L/D = 190$ at the onset to slug flow for $U_{SG} = 5.5$ m/s.

slug flow are too high when compared to experimental data. This is indicated in Fig. 14(b) which shows experimental and predicted values of U_{SL} required to initiate slug flows for $\theta = -0.5^{\circ}$. The viscous analysis of Lin and Hanratty provides the best agreement with the experimental data. Thus, the stability of the observed long wavelength waves define the transition to slug flow.

For flow conditions prior to the observation of slugs in declined flows, growth of long wavelength waves is observed. Since the growth of these waves is small, slug flows are expected to be observed at values of U_{SL} slightly below the transition boundary shown in Fig. 2 if a longer pipeline were used in the experiments. Consequently, the lower curve in Fig. 14 should define the initiation of slug flows in very long pipelines.

The calculations in Fig. 14 were carried out by assuming a flat profile. Shape factors are defined as

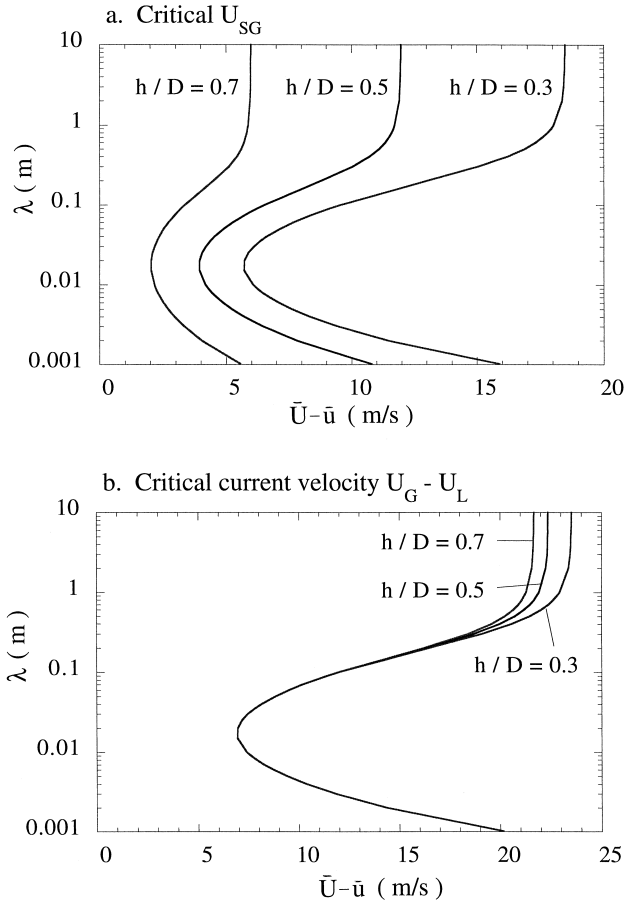

Fig. 13. Neutral stability curves using an inviscid analysis.

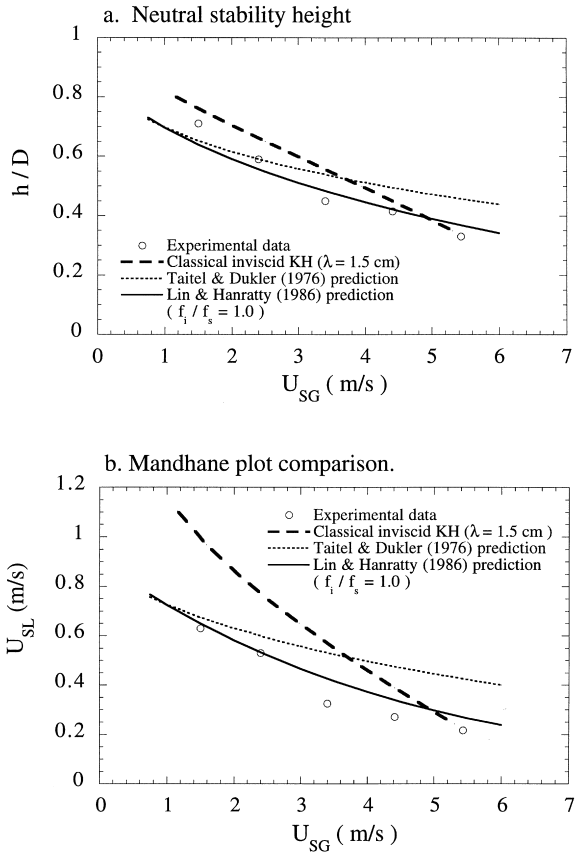

Fig. 14. Comparison of neutral stability predictions with experimental data ($D = 0.0763$ m/s, $\theta = -0.5°$).

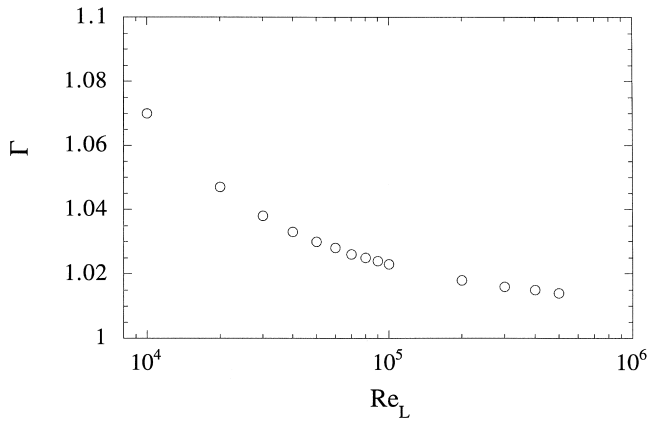

Fig. 15. Shape factor as a function of Re_L.

$$\Gamma = \frac{1}{\bar{u}A_{2_L}} \int u^2 \, dA \tag{31}$$

where $\Gamma = 1$ corresponds to a plug flow. Values of Γ are plotted in Fig. 15. Details of this calculation are given in the thesis of Woods (1998). Lin and Hanratty have shown that an approximate correction can be made to Eq. (14) to account for the errors in assuming a plug flow, by making the following substitution:

$$\left(\frac{C_R}{\bar{u}} - 1\right)^2 \rightarrow \left(\frac{C_R}{\bar{u}}\right)^2 - 2\Gamma\left(\frac{C_R}{\bar{u}}\right) + \Gamma \tag{32}$$

This correction is used in the comparison of measurements with the long wavelength viscous stability analysis in Fig. 16. Values of f_i/f_s used in these calculations were obtained from experiments. The long wavelength theory on viscous instability is found to provide a good prediction for the onset of slugging for all of the values of θ that were studied.

Values of C_R obtained from the long wavelength theory are compared with measurements in Fig. 17. Perfect agreement cannot be expected since observations necessarily require finite amplitude waves. For inclined flows these are the velocities of the long wavelength waves, obtained from cross correlation measurements, such as shown in Fig. 9. Value of C_R for horizontal flows represent the $f = 5$ Hz waves observed at the onset of slugging.

Shoham (1982) studied air–water flows in inclined and declined pipes with diameters of 2.5 and 5.1 cm. Fig. 18 compares Shoham's observations of the transition from stratified to slug flow with the long wavelength stability analysis. Reasonably good agreement between theory and experiments is obtained using $\Gamma = 1$ and $f_i/f_s = 1.0$.

6. Summary and conclusions

Results from this study show that waves of the type observed by Fan et al. (1993a, 1993b) in

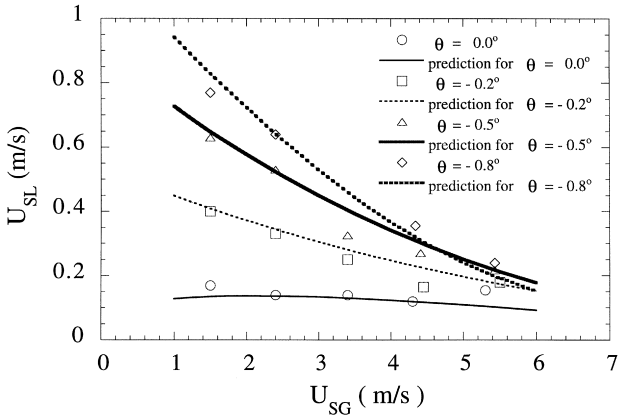

Fig. 16. Comparison of viscous linear stability predictions of values of U_{SL} needed to initiate slug flows with experimental data ($\bar{\Gamma} \neq 1, f_i/f_s \neq 1$).

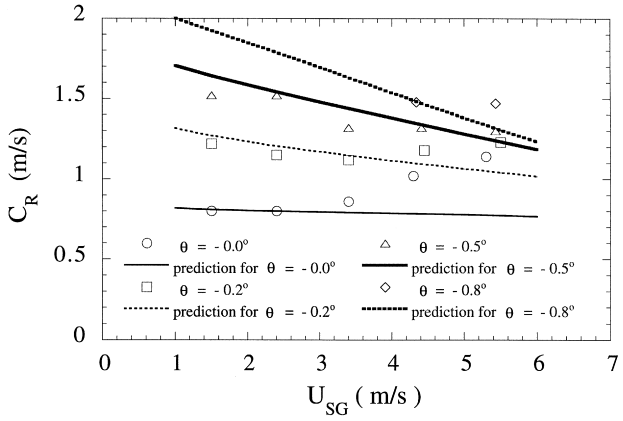

Fig. 17. Comparison of viscous linear stability predictions of the wave velocity C with experimental data ($\bar{\Gamma}\neq 1, f_i/f_s \neq 1$).

a horizontal pipe are completely suppressed at -0.2°, as has been previously reported by Andreussi and Persen (1987). The transition to slug flow was found to be associated with the appearance of very long wavelength waves ($\lambda \cong 5$–10 m); the frequency of slugging is equal to the frequency of these waves. The transition to slugging is found to be described by a viscous long wavelength analysis that directly accounts for the influence of declination. Photographic studies of the transition process support the suggestion of Kordyban (1985) that actual slug initiation occurs through a local Kelvin–Helmholtz instability of small wavelength waves on the crest of long wavelength waves. Thus, the instability is triggered by the long wavelength waves. This result could provide a resolution of the paradox presented by the measurements of Fan et al. (1993a, 1993b) in a horizontal pipe.

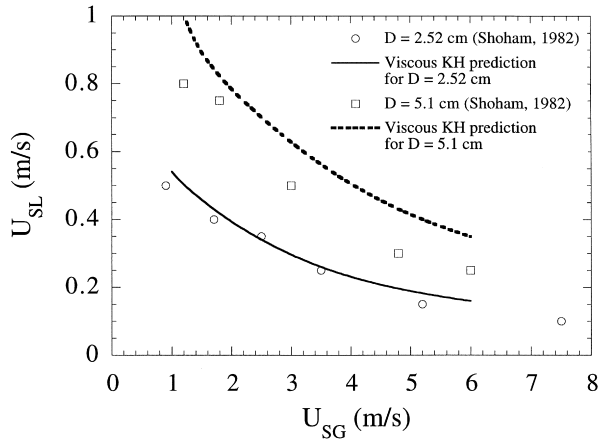

Fig. 18. Comparison of viscous linear stability predictions with results of Shoham (1982) for $\theta = -1.0^\circ$.

Acknowledgements

Acknowledgement This work is supported by the Department of Energy under Grant DOE DEF 86ER 13556.

References

Andreussi, P., Persen, L.N., 1987. Stratified gas–liquid flow in downwardly inclined pipes. Int. J. Multiphase Flow 13, 565–575.

Barnea, D., Shoham, O., Taitel, Y., Dukler, A.E., 1980. Flow pattern transition for gas–liquid flow in horizontal and inclined pipes. Int. J. Multiphase Flow 6, 217–225.

Fan, Z., Lusseyran, F., Hanratty, T.J., 1993a. Initiation of slugs in horizontal gas–liquid flows. AIChE J 39, 1741–1753.

Fan, Z., Ruder, Z., Hanratty, T.J., 1993b. Pressure profiles for slugs in horizontal pipelines. Int. J. Multiphase Flow 19, 421–437.

Govier, G.W., Aziz, K., 1972. The Flow of Complex Mixtures in Pipes. Van Nostrand Reinhold, NY, p. 562.

Grolman, E., Commandeur, N., de Baat, E., Fortuin, J., 1996. Wavy-to slug flow transition in slightly inclined gas–liquid pipe flow. AIChE J 42, 901–907.

Kokal, S.L., Stanislav, J.F., 1989. An experimental study of two-phase flow in slightly inclined pipes. Part II: Liquid holdup and pressure drop. Chem. Engng. Sci 44, 681–693.

Kordyban, E.S., 1985. Some details of developing slugs in horizontal two phase flow. AIChE J 31, 802–806.

Kordyban, E.S., Ranov, T., 1970. Mechanism of slug formation in horizontal two-phase flow. J. Basic Engng 92, 857–864.

Lin, P.Y., Hanratty, T.J., 1986a. Prediction of the initiation of slugs with linear stability theory. Int. J. Multiphase Flow 12, 79–98.

Lin, P.Y., Hanratty, T.J., 1986b. Detection of slug flow from pressure measurements. Int. J. of Multiphase Flow 13, 13–21.

Lighthill, M.J., Whitham, G.B., 1955. On kinematic waves. Part I: Flood movement in long rivers. Part II: Theory of traffic flow on long crowded roads. Proc. Roy. Soc A 229, 281–345.

Milne-Thomson, L.M. 1980. In: Theoretical Hydrodynamics, 5th ed. MacMillan, London.

Shoham, O., 1982. Flow pattern transitions and characterization in gas–liquid flow in horizontal pipes. Ph.D. Thesis, Tel-Aviv University, Israel.

Stanislav, J.F., Kokal, S., Nicholson, M.K., 1986. Intermittent gas–liquid flow in upward inclined pipes. Int. J. Multiphase Flow 12, 325–335.

Taitel, Y., Dukler, A.E., 1976. A model for predicting flow regime transitions in horizontal and near horizontal gas–liquid flow. AIChE J 22, 47–55.

Wallis, G.B., Dobbins, J.E., 1973. The onset of slugging in horizontal stratified air–water flow. Int. J. Multiphase Flow 1, 173–193.

Williams, L.R., 1990. Effect of pipe diameter on horizontal annular two phase flow. Ph.D. Thesis, University of Illinois, Urbana.

Woods, B.D., 1998. Slug formation and frequency of slugging in gas–liquid flows. Ph.D. Thesis, University of Illinois, Urbana.

Woods, B.D., Hanratty, T.J., 1996. Relation of slug stability to shedding rate. Int. J. Multiphase Flow 22, 809–828.

Wu, H.L., Pots, B.F.M., Hollenburg, J.F., Merhoff, R., 1987. Flow pattern transitions sin two-phase gas/condensate flow at high pressure in an 8-inch horizontal pipe. In: Proc. BHRA Conf., The Hague, The Netherlands, 13–21.